ELSEVIER

Studies on the solution conformation and dynamics of a polysaccharide from *Sinorhizobium fredii* HH103 and its monosaccharide repeating unit

Miguel A. Rodríguez-Carvajal,* Manuel Bernabe,† José L. Espartero,‡ Pilar Tejero-Mateo,* Antonio Gil-Serrano,* and Jesús Jiménez-Barbero†

**Departamento Química Orgánica, Facultad Química, University of Sevilla, Sevilla, Spain*
†Instituto Química Orgánica, CSIC, Madrid, Spain
‡Dpto. Química Orgánica y Farmacéutica, Facultad Farmacia, University of Sevilla, Sevilla, Spain

The conformational behavior of the homopolysaccharide isolated from Sinorhizobium fredii HH103 and its monosaccharide repeating unit (5-acetamido-3,5,7,9-tetradeoxy-7-(3-hydroxybutyramido)-L-glycero-L-manno-nonulosonic acid) was analyzed by nuclear magnetic resonance (NMR) spectroscopy and extensive molecular dynamics simulations (MD). The results indicate that the glycosidic linkages and lateral chains may adopt a variety of conformations. MD simulations using the generalized Born solvent-accessible surface area (GB/SA) continuum solvent model for water and the MM3 force field provide a population distribution of conformers that satisfactorily agrees with the experimental NMR data for the torsional degrees of freedom of the molecule. © 2000 by Elsevier Science Inc.*

Keywords: K-antigen, NMR, molecular dynamics, polysaccharide, pseudaminic acid

INTRODUCTION

Sinorhizobium fredii is a gram-negative soil bacterium that induces nodules on the roots of different legumes, such as *Glycine max* (soybean). Within these nodules, the bacteria fix atmospheric nitrogen. Many nodulation genes are involved in the synthesis and secretion of lipo-chitin oligosaccharides, known as LCOs or Nod factors.[1] In addition to bacterial genes involved in nitrogen fixation, other determinants are required for formation of a functional nodule. These determinants include certain polysaccharides: β-glucans, acidic exopolysaccharides (EPS), capsular polysaccharides (CPS), and lipopolysaccharides (LPS).[2] In the genus *Rhizobium*, the outer membrane and the surrounding capsule are composed of a complex array of LPS and a Kdo- or Kdo-related containing polysaccharide, structurally analogous to the constituents of the group II K-antigen polysaccharides of *Escherichia coli.*

We recently reported on the primary structure of a K-antigen capsular polysaccharide that is not in agreement with the consensus structure.[3] It consists of a homopolymer of 5-acetamido-3,5,7,9-tetradeoxy-7-[(*R*)- and (*S*)-3-hydroxy-butyramido]-L-*glycero*-L-*manno*-nonulosonic acid. The sugar residues are attached via a glycosidic linkage to the OH group of the 3-hydroxybutyramido moiety; thus, the monomers are linked via both glycosidic and amido linkages. Seventy-five percent of the 3-hydroxybutyramido shows the *R*-configuration.

We now report on the solution conformation and dynamics of this unusual polysaccharide and its monosaccharide repeating unit, using nuclear magnetic resonance (NMR) techniques and molecular dynamics (MD) calculations.[4,5] Given the putative flexible nature of the polysaccharide, the combination of NMR and modeling is needed to deduce realistically the conformational properties of the macromolecule.[6] Both the conformation of the pyranose rings and the orientation around the glycosidic and additional linkages have been analyzed.

MOLECULAR MECHANICS AND DYNAMICS CALCULATIONS

Building Monosaccharide and Oligosaccharide Structures

Molecular mechanics and dynamics calculations were performed using the MM3* force field[7] as implemented in MAC-

Color Plates for this article are on page 166.

Corresponding author: Jesús Jiménez-Barbero, Instituto Química Orgánica, CSIC, Juan de la Cierva 3, Madrid, 28006-Spain. Tel.: 34-1-5622900X225; fax: 34-1-5644853

E-mail address: iqoj101@iqog.csic.es (J. Jiménez-Barbero)

655 Avenue of the Americas, New York, NY 10010

1093-3263/00/$–see front matter
PII S1093-3263(00)00045-0

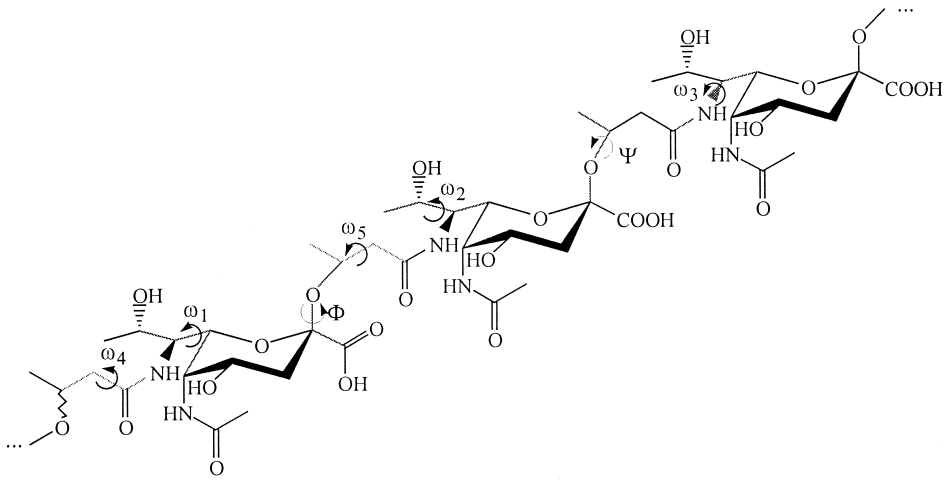

Scheme 1. Schematic view of the polysaccharide showing the relevant torsion angles.

ROMODEL 4.5.[8] Φ is defined as Pseu-C1 Pseu-C2 Pseu-O2 But-C3′ and Ψ as Pseu-C2 Pseu-O2 But-C3′ But-C4′. Other torsion angles are defined as ω_1 as Pseu-C5 Pseu-C6 Pseu-C7 Pseu-C8, ω_2 as Pseu-C6 Pseu-C7 Pseu-C8 Pseu-C9, ω_3 as Pseu-C6 Pseu-C7 But-N7 But-C1′, ω_4 as But-N7 But-C1′ But-C2′ But-C3′, and ω_5 as But-C1′ But-C2′ But-C3′ But-C4′. A schematic view is given in Scheme 1. Twenty-seven starting geometries were selected as follows: ω_1 and ω_2 were set as 180 and −60°, according to the NMR data (see Results and Discussion), although these two angles were let free during the minimizations and MD simulations. The three possible staggered orientations of ω_3, ω_4, and ω_5 torsions were combined to give the 27 (×2) initial conformations of the monosaccharide with the butyramido moiety having the *R*- and *S*-configurations. The torsion angles for ω_3, ω_4, and ω_5 are termed g+, g−, or anti, representing angles in the proximity of +60, −60, or 180°.

Molecular Mechanics Calculations

Minimizations were performed for the *S*- and *R*-configurations of the butyramido chain. The amide linkages were built in their usual *trans* conformations. Calculations for a dielectric constant $\epsilon = 80$ and for the continuum generalized Born solvent-accessible surface area (GB/SA) solvent model[9] (MM3*) were performed. Using both GB/SA and a bulk dielectric constant of $\epsilon = 80$ has been reported to reproduce satisfactorily the conformational behavior of carbohydrate derivatives in water solution.[10] First, the 27×2 structures were minimized with 5000 conjugate gradient iterations or until root mean square (RMS) derivative was less than 0.05 kcal mol^{-1} Å^{-1}. In addition to the separated minimizations, relaxed energy maps for ω_4/ω_5 combinations were calculated. These calculations were carried out with initial geometries of $\omega_1 = 180°$, $\omega_2 = -60°$, and $\omega_3 = -120°$ for the respective torsion angles. The previous step involved the generation of corresponding rigid residue maps using a grid step of 18°. Every (ω_4, ω_5) point of this map was optimized using 2500 conjugate gradient iterations. Following this protocol, the maximum RMS derivative was less than 0.06 kcal mol^{-1} Å^{-1}. From these relaxed maps, probability distributions were calculated for each point according to a Boltzmann function at 303K. From the maps and the individual 54 minimizations, probability distributions for the lateral chain orientations were calculated. From the more probable conformations, two starting structures of a disaccharide and two of a tetrasaccharide model of the polysaccharide were built and subjected to extensive energy minimization until the RMS gradient was less than 0.05 kcal mol^{-1} Å^{-1}.

MD Simulations

The 27 (×2) final structures of the minimizations of the monosaccharide geometries were used as starting geometries for MD simulations at 300K, and their results were carefully analyzed. Average torsions and proton–proton distances were calculated from the MD simulations.

The minimized disaccharide and tetrasaccharide structures were used as starting geometries for MD simulations at 300K. For both the monosaccharides and the oligosaccharides, separate calculations were performed using the GB/SA solvent model for water and a bulk dielectric constant of 80. For all molecules, the simulations were carried out at a time step of 1 fs. The equilibration period was 100 ps. Structures were saved every 1 ps. The total simulation time was 0.5 ns for every run. Average distances between proton pairs were calculated from the MD simulations.[11]

NMR SPECTROSCOPY

NMR experiments were recorded on a Varian Unity 500 spectrometer, using an approximately 12 mM solution of the monosaccharide and a 2 mg/mL solution of the polysaccharide at different temperatures (between 299K and 320K). The spectra were recorded in D_2O. Chemical shifts are reported in ppm, using external DSS (0 ppm) as reference. The double quantum filtered COSY spectrum was performed using 256 increments of 1K real points to digitize a spectral width of 2000 Hz. Sixteen scans were used with a relaxation delay of 1 s. The 2D TOCSY experiment was performed using a data matrix of 256 increments of 1K real points to digitize a spectral width of 2000 Hz. Four scans were used per increment with a relaxation delay of 2 s. MLEV 17 was used for the 100-ms isotropic mixing time. The one-bond proton-carbon correlation experiment was collected using the gradient-enhanced HSQC sequence.[12] A

Table 1. ^{1}H and ^{13}C NMR Chemical Shifts (δ, ppm) of the Monosaccharide and Polysaccharide[3]

Atom (H, C)	Pseu (poly)	But	Pseu (mono)	But	Pseu (poly)	But	Pseu (mono)	But
1	—	—	—	—	173.7	178.0	175.0	177.4
2	—	2.57, 2.43	—	2.41, 2.39	99.7	45.2	97.7	46.4
3	1.52, 2.11	4.20	1.81, 1.94	4.23	37.2	68.0	36.0	66.2
4	4.20	1.21	4.18	1.26	66.4	19.9	66.6	23.4
5	4.21	2.01*	4.25	2.03*	49.8	175.7*	50.1	175.9*
6	4.07		4.06		73.1	23.4*	71.3	23.2*
7	4.19		4.19		55.1		54.2	
8	4.30		4.14		69.2		68.4	
9	1.30		1.13		18.3		16.8	

* Assignments for the *O*-acetyl group.

data matrix of 256 increments of 1K real points was used to digitize a spectral width of 2000 Hz in F_2 and 10,000 Hz in F_1. Four scans were used per increment with a relaxation delay of 1 s and a delay corresponding to a J value of 145 Hz. ^{13}C decoupling was achieved using the WALTZ scheme. The 2D-HMQC-TOCSY experiment was conducted with an 80-ms mixing time (MLEV 17). The same conditions as for the HSQC experiment were employed. HMBC experiments were performed using the gradient-enhanced sequence[13] with 256 increments of 2K real points to digitize a spectral width of 2000 $\times$ 15,000 Hz. Eight scans were acquired per increment with a delay of 65 ms for evolution of long-range couplings.

The 2D NOESY,[14] 2D-ROESY,[15] and 2D-T-ROESY[16] experiments were performed using four different mixing times, i.e., a50, 300, 450, and 600 ms, with 256 increments of 2K real points. Good linearity was observed up to 200 ms (NOESY) and 300 ms (ROESY). Estimated errors in the NOE intensities are less than 20%. The 1D-NOESY experiments using the double pulse field gradient spin-echo technique[17] were acquired with the same mixing times.

RESULTS AND DISCUSSION

^{1}H NMR Data

Because NMR parameters are averaged over time and on many molecules, the information that can be deduced from these experiments corresponds to the time-averaged conformation of the monosaccharide and polysaccharide in solution. ^{1}H NMR and ^{13}C NMR spectra of the monosaccharide and the polysaccharide were completely assigned[3] by a combination of homonuclear COSY, TOCSY, and heteronuclear HMQC, HMBC, and HMQC-TOCSY techniques. The last two techniques were crucial to solving the final ambiguities. The corresponding ^{1}H and ^{13}C NMR chemical shifts are listed in Table 1.

The pyranose six-membered rings can be described as essentially monoconformational: $^1C_4$, as deduced from the vicinal proton–proton couplings[18] (Table 2). For the monosaccharide, the couplings for the C6-C9 lateral chain defined by ω_1 and ω_2 were $J_{6,7}$ 10.5 Hz and $J_{7,8}$ 3.3 Hz, indicating a major conformation of the lateral chain, which is in agreement with a *trans*-like relationship between H-6 and H-7 and a *syn*-type orientation between H-7 and H-8. The C8-C9 bond is flexible, as deduced by the averaged $J_{8,9}$ coupling constant value of 6.5 Hz.

The coupling values in the polysaccharide were estimated from the line widths in TOCSY, COSY ,and ^{1}H-coupled HSQC experiments. It can be deduced that the magnitudes of $J_{6,7}$, $J_{7,8}$, and $J_{8,9}$ did not change appreciably for the polymer, indicating a similar set of torsion angles. The NOESY/ROESY experiments that were performed with different mixing times were used to estimate proton–proton interresidue distances.[19] The good linearity observed in the build-up curves for NOESY/ROESY spectra warranted the safe application of the isolated spin pair approximation, within certain bounds. For the monosaccharide, all NOESY cross peaks were positive (data not shown) at 500 MHz and 299 K. For the polysaccharide (Figure 1), the corresponding cross peaks were negative, as expected for a slow tumbling molecule. The resulting distances are given in Table 3. The Pseu H-3ax/H-3eq intraresidue signals were used as a reference, assuming their separation is 1.78 Å. Thus, the NOEs were first assigned as strong (s), medium (m), and weak (w) and then quantitated. The MD-calculated distances (see later) are shown in Table 3. It can be observed that there is a good match between the experimental distances and those estimated through molecular mechanics and dynamics simulations. The data from the NOESY and ROESY experiments also are in agreement with the J data, and the complete set of observed data indicated the existence of conformational equilibria in all cases.

Table 2. Vicinal Proton–Proton Coupling Constants[3] for the Monosaccharide (Hz)

Vicinal coupling	Butyryl	Pseu*p*
H-1/H-2	—	—
H-2/H-3	8.1, 4.9	
H-3/H-4	6.3	12.7, 5.0
H-4/H-5		4.2
H-5/H-6		1.7
H-6/H-7		10.5
H-7/H-8		3.3
H-8/H-9		6.5

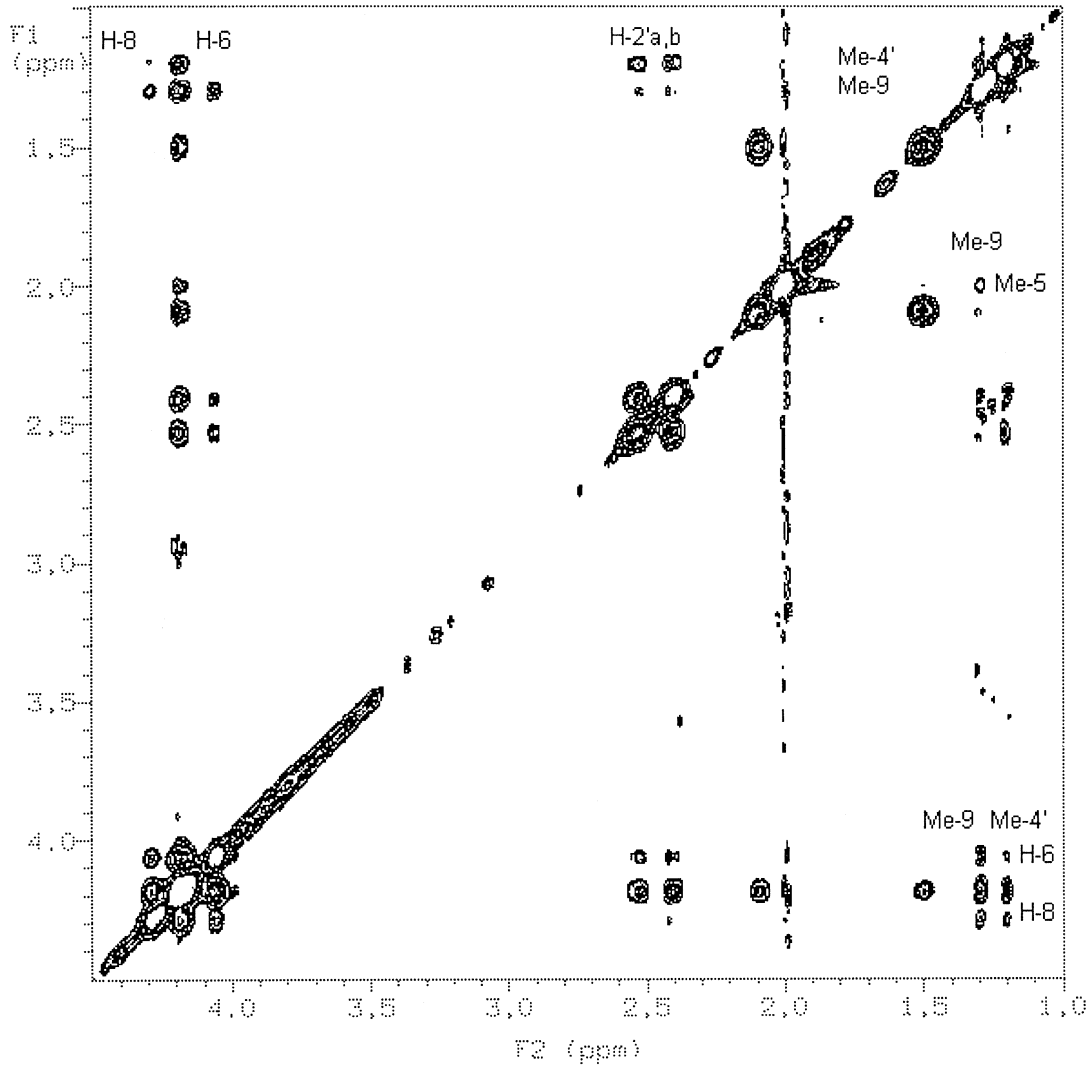

Figure 1. Partial section of a 500-MHz NOESY of the polysaccharide at 299K. Mixing time = 300 ms.

Conformational Analysis: MD Studies

The monosaccharide: starting conformations and conformational distributions

As a first step in determining the overall three-dimensional structure of the polysaccharide, molecular mechanics and dynamics calculations were performed on the monosaccharide.

Table 3. Experimental nontrivial NOEs for the polysaccharide *Vs* the MM-simulated interresidue H/H distances for the octasaccharide and the average values obtained from MD of the tetrasaccharide

H/H PAIR	MM	MD	NOE	EXP
Pseu 9/Pseu 6*	1.9	1.7 (1.4/2.2)	s	2.5–2.9
Pseu 8/Pseu 6*	3.0	3.0 (2.4/3.7)	s	2.5–2.9
But 4/Pseu 6	1.6	3.3 (1.7/5.4)	w	2.9–3.5
But 4/Pseu 8	2.2	3.6 (2.5/5.0)	mw	2.8–3.4
Pseu 9/But 2a, b	3.4	3.5 (2.5/5.0)	m	2.7–3.3
Pseu 9/Ac-Me	2.3	4.0 (2.2/8.3)	w	2.9–3.5
Pseu 6/But 2a, b	4.3	3.8 (1.8/5.3)	mw	2.8–3.4
Pseu 7/But 2a, b	3.6	4.6 (3.4/6.9)	w	2.9–3.5

The average values found during the molecular mechanics (MM) calculation for the different glycosidic linkages are given. For methyl groups, the H/H distances were calculated subtracting 1.1 Å from the corresponding carbon—proton distance.
* NOEs also observed in the monosaccharide.
The NOE intensities are denoted as w (weak), m (medium), and s (strong).

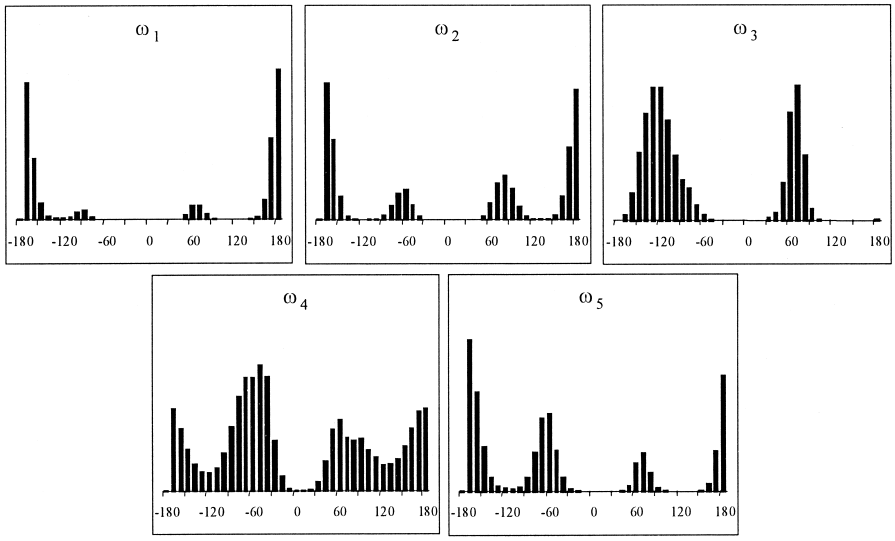

Figure 2. Histogram of the populations of the different torsion angles of the monosaccharide during the 27 ns MD simulation with the MM3 force field.*

After MM3* minimization of the starting 27 (×2) geometries, information on the conformational space accessible was obtained by MD simulations[20] of the monosaccharide using the MM3* program.[10] In particular, the MD simulations were performed using the 54 output geometries of the molecular mechanics calculations as starting structures (see earlier). Thus, different ω_i torsions, and both *S*- and *R*- configurations of the butyramido chain, were considered. A summary of the MD results presented as a histogram of the torsion angle values is shown in Figure 2. As can be observed, ω_1 remained close to 180°, in all simulations. For ω_2, the three staggered conformations are possible according to MD, although the experimental data indicate that a major conformation close to −60° should be present. Otherwise, a much higher $J_{7,8}$ should be observed. Two clusters of values are observed for ω_3. In one cluster, this torsion angle adopts a value around +60°. In the second cluster, the angle changes to −120°, thus providing a much smaller relative steric energy value. For ω_4 and ω_5, the computed dihedral angle values seem to be correlated. Thus, the couples ω_4/ω_5 −60°/180°, 60°/60°, −60°/−60°, and 180°/−60 frequently are observed independently of the starting structure and correspond to low-energy minima. To analyze these values properly, potential energy maps were calculated for the monosaccharides with *S* and *R*-configurations in the butyramido moieties. Relaxed (ω_4,ω_5) potential energy maps also were calculated as described.[10] The maps obtained were almost identical, and the minima found in these maps closely corresponded to those observed in the MD. The global minimum, as well as other low-energy minima, are presented in Table 4.

Although the presence of other conformers cannot be discarded and it is possible that several geometries are present simultaneously, a representative view of the major conformation of the monosaccharide, which agrees with the molecular mechanics and dynamics calculations and with the NMR data, is shown in Color Plate 1.

Toward a model of the polysaccharide: building and study oligomeric fragments

Once the monosaccharide (*R*- and *S*-) repeating units had been analyzed, two disaccharide units were built from the monosaccharide global minima, extensively minimized, and used to generate models of a tetrasaccharide molecule, first having the *R*-configuration for all four 3-hydroxybutyramido groups. These geometries were minimized and then submitted to one MD simulation. The initial conformation of the lateral chains was selected to agree with the experimental data (see Table 3 for a comparison between experimental and MD results). From the MD, it can be observed that the *exo*-anomeric orientation[21] around Φ (Φ = 60°) is primarily adopted. With regard to Ψ, a major *syn* relationship between the six-membered ring and the lateral chain is adopted, with values around −120° (Figure 3). These values involve a nearly

Table 4. Global Minimum and Main Low-Energy Minima Found in the Molecular Mechanics Minimizations and in the Relaxed Potential Energy Maps for the Monosaccharide

R						*S*					
ω_1	ω_2	ω_3	ω_4	ω_5	E (kJ/mol)	ω_1	ω_2	ω_3	ω_4	ω_5	E (kJ/mol)
−179	−65	−138	−77	180	105.8	−178	−65	−135	−72	−175	105.4
−178	−63	−134	71	175	106.7	−180	−64	−131	−174	−178	106.5
−179	−65	−133	178	177	107.2	−179	−65	−135	74	179	107.2
−178	−67	−145	−77	−59	107.9	−179	−66	−143	−78	−66	108.1
−179	−65	−135	73	62	108.9	−178	−65	−135	70	54	108.8

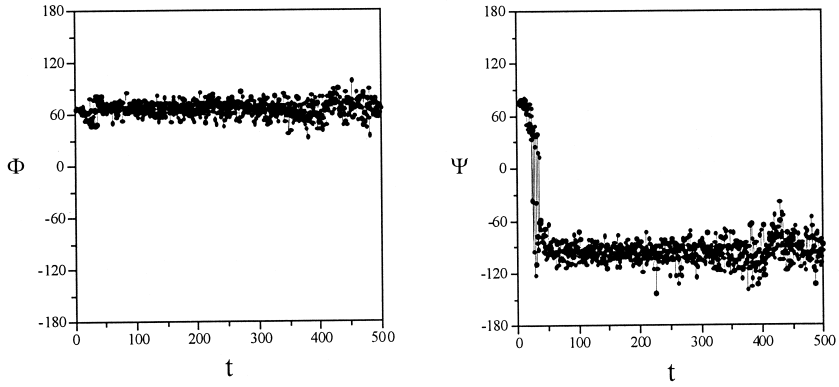

Figure 3. Trajectory plots of Φ/Ψ glycosidic torsion angles for linkages during a 0.5 ns MD simulation for the tetrasaccharide with the MM3 force field. All three pairs Φ/Ψ, one for each glycosidic linkage, are shown. An extended surface around the corresponding global minima is occupied during the simulation.*

Table 5. Torsion Angles for the Minimized Structure of the Octasaccharide and Average Values Obtained from MD of the Tetrasaccharide

Torsion	MD tetra average	Octa average
Φ	66	67
Ψ	−86	76
ω_1	175	174
ω_2	−72	−77
ω_3	−137	−137
ω_4	−168	−168
ω_5	74	65

eclipsed disposition between the bonds C2-O2 and C3′-H3′, thus minimizing the steric interactions between the sugar ring and both the methyl group and the rest of the side chain. In all cases, the torsional oscillations were more pronounced around Ψ,, which is as expected because the *exo*-anomeric effect restricts Φ. With respect to *ω* torsions, although, according to the simulations, a variety of possibilities could occur, the most stable one by far corresponds to ω_1 anti, ω_2 g−, ω_3 −120, ω_4 anti, and ω_5 g+. Thus, the different possibilities for ω_4 and ω_5 in the monosaccharide are constrained to a major one in the polysaccharide. All the energy regions show Φ values (Table 5) that are centered around those expected for the *exo*-anomeric effect.[21]

Comparison of the deduced NMR-derived distances and those predicted by molecular mechanics is presented in Table 3. In the same way, the average expected interproton distances from the MD simulation were estimated and compared to those observed experimentally (Table 3). Although the corresponding average structure can explain satifactorily most of the observed interresidue NOEs for the polymer, some of the values found in the MD differ from the experimental data, especially the Me-9/Me-Ac distance.

To determine an explanation this discrepancy, a second tetrasaccharide was built that used two different disaccharidic repeating units. The first has a hydroxybutyramido residue with the *S*-configuration at the nonreducing end and the second with the *R*-configuration at the reducing end. This tetrasaccharide, termed *SRSR*, was submitted to MD simulation. In this case, it can be observed that the values for Ψ and ω_5 are very different, depending on the configuration of the hydroxybutiramido group involved in glycosidic linkage. Ψ values around −120° and ω_5 values around 60° were observed for the *R*-configuration, and Ψ values around 120° and ω_5 around −60° were observed for the *S*-configuration (Figure 4). In both cases, orientation between the bonds C2-O2 and C3′-H3′ is near eclipsed, and the orientation between the bonds C1′-C2′ and C3′-O2 is *anti*.

Regarding the calculated interproton distances, the trajectory plots for the Me-9/Ac-Me distance for the *SRSR* tetrasaccharide are shown in Figure 5. It can be observed that both methyl groups come close in space during the whole MD simulations. Thus, the corresponding NOE signals may be safely be explained by considering a homogeneous distribution of both *R*- and *S*-configurations of the hydroxybutyramido groups along the polysaccharide chain.

Superimposition of different conformers found in the MD

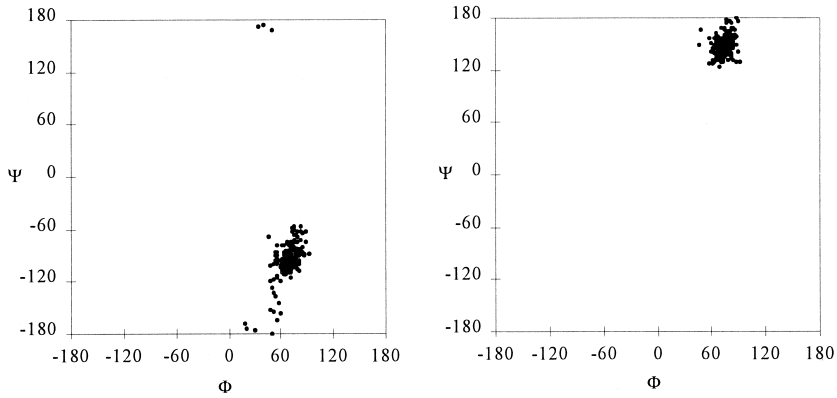

Figure 4. Plots of Φ/Ψ glycosidic torsion angles for linkages between the ring sugar and an R*-configuration hydroxybutyramido (left) and an* S*-configuration hydroxybutyramido (right) during a 0.5 ns MD simulation for the tetrasaccharide* SRSR *with the MM3* force field.*

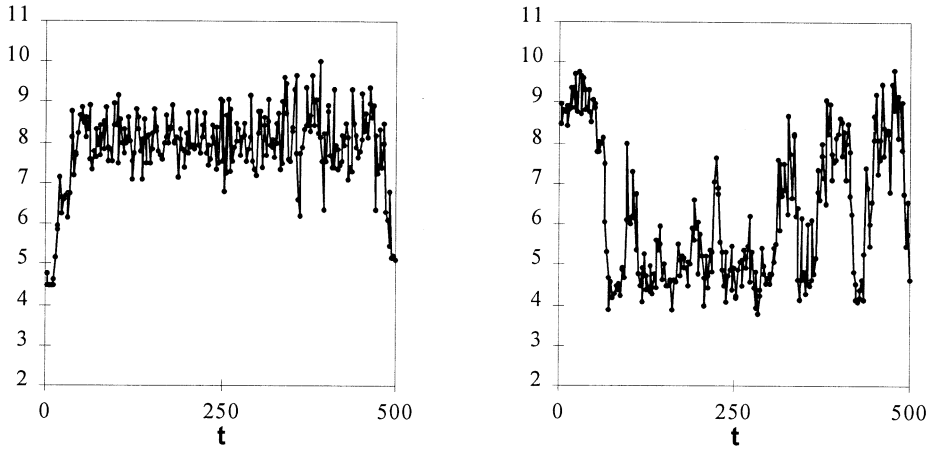

Figure 5. Trajectory plots of C9/Ac-Me distances of the tetrasaccharide RRRR *(left) and* SRSR *(right), which may be correlated with NOEs during one MD simulation with the MM3* force field.*

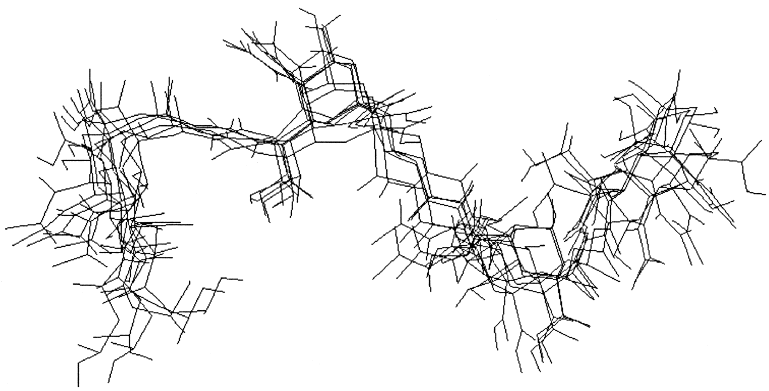

Figure 6. Superimposition of different conformers of the tetrasaccharide SRSR*, found during one MD simulation.*

simulation of the tetrasaccharide *SRSR* is shown in Figure 6. Despite the relatively narrow variation of the glycosidic torsion angles, the conformational space accessible to the tetrasaccharide may be fairly large.

Similarly, to examine the behavior of these torsion angles in larger structures, an octasaccharide was built and submitted to minimization. The conformation was fairly stable, as the resulting torsion angles did not differ greatly from the starting values. The corresponding interproton distances and torsion angles are given in Tables 3 and 5. A view of a putative conformation of the corresponding all*R*-oligosaccharide is shown in Color Plate 2. It can be observed that the chain may adopt a pseudohelical structure, which also may explain satisfactorily the observed NOEs.

CONCLUSION

Summarizing the experimental and computational results, there appears to be an important amount of conformational freedom for the glycosidic and exocyclic torsion angles of the polysaccharides. Unrestrained molecular mechanics and MD simulations provide a picture that agrees satisfactorily with the NMR experimental data when a homogeneous distribution of lateral chains having the *R*- and *S*-configurations is considered. It can be deduced from these data that the nature of the receptor binding sites can easily modulate the conformational behavior of this molecule.

ACKNOWLEDGMENTS

Financial support by DGICYT (Grants PB96-0833 and BIO96-1469-C03) is gratefully acknowledged. We thank Dr. J.E. Ruiz-Sainz, Departamento de Microbiología, Facultad de Biología, Universidad de Sevilla, for supplying bacterial cultures.

REFERENCES

1 Wilkinson, S.G. *Prog. Lipid. Res.* 1996, **35,** 283
2 Becker, A., and Pühler, A. In *The Rhizobiaceae*, Spaink, H.P., Kondorosi, A., and Hooykaas, P.J.J., Eds., Kluwer Academic Publishers, Dordrecht, 1998
3 Gil-Serrano, A.M., Rodríguez-Carvajal, M.A., Tejero-Mateo, P., Espartero, J.L., Menéndez, M., Ruiz-Sainz, J.E., and Buendía-Claveria, A.M. *Biochem. J.* 1999, **342,** 527–535
4 (a) Rutherford, T. J., Spackman, D.G., Simpson, P.J., and Homans, S.W. *Glycobiology* 1994, **4,** 59. (b) Poveda, A., Asensio, J.L., Martin-Pastor, M., and Jimenez-Barbero, J. *J. Chem. Soc., Chem. Commun.* 1996, 421. (c) Harris, R., Kiddle, G.R., Field, R.A., Milton, M.A., Ernst, B., Magnani, J.L., and Homans, S.W. *J. Am. Chem. Soc.* 1999, **121,** 2546–2551
5 (a) Meyer, B. *Topics Curr. Chem.* 1990, **154,** 141. (b) Bock, K. *Pure Appl. Chem.* 1983, **55,** 605. (c) Imberty, A. *Curr. Opin. Struct. Biol.* 1997, **7,** 617–623. (d) Peters, T., and Pinto, B.M. *Curr. Opin. Struct. Biol.* 1996, **6,** 710–720

6 (a) Imberty, A., Hardman, K.D., Carver, J.P., and Perez, S. *Glycobiology* 1991, **1,** 456. (b) Espinosa, J.F., Cañada, F.J., Asensio, J.L., Martín-Pastor, M., Dietrich, H., Martín-Lomas, M., Schmidt, R.R., and Jiménez-Barbero, J. *J. Am. Chem. Soc.* 1996, **118,** 10862–10871. (c) Dowd, M.K., Reilly, O.J., and French, A.D. *Biopolymers* 1994, **34,,** 625–638
7 Allinger, N.L., Yuh, Y.H., and Lii, J.H. *J. Am. Chem. Soc.* 1989, **111,** 8551. The MM3* force field implemented in MACROMODEL differs from the regular MM3 force field in the treatment of the electrostatic term because it uses charge–charge instead of dipole–dipole interactions
8 Mohamadi, F., Richards, N.G.I., Guida, W.C., Liskamp, R., Canfield, C., Chang, G., Hendrickson, T., and Still, W.C. *J. Comput. Chem.* 1990, **11,/BLD 440**
9 Still, W.C., Tempczyk, A., Hawley, R.C., and Hendrickson, T. *J. Am. Chem. Soc.* 1990, **112,** 6127
10 (a) Martín-Pastor, M., Espinosa, J.F., Asensio, J.L., and Jimenez-Barbero, J. *Carbohydr. Res.* 1997, **298,** 15–47. (b) Coteron, J.M., Singh, K., Asensio, L., Dalda, M.D., Fernández-Mayoralas, A., Jiménez-Barbero, J., and Martín-Lomas, M.*J. Org. Chem.* 1995, **60,** 1502–1513. (c) Espinosa, J.F., Asensio, J.L., Bruix, M., and Jimenez-Barbero, J. *An. Quim. Int. Ed.* 1996, **6,** 320–324. (d) Asensio, J.L., Martin-Pastor, M., and Jimenez-Barbero, J. *J. Mol. Struct.* 1997, **395–396,** 245–270
11 For a relevant survey of the application of molecular mechanics and dynamics simulations to carbohydrate molecules, see French, A.D., and Brady, J.D., Eds. *Computer modelling of carbohydrate molecules,* ACS Symposium Series 430, American Chemical Society, Washington, DC, 1990
12 Boyd, J., Soffe, N., John, B., Plant, D., and Hurd, R. *J. Magn. Reson.* 1992, **98,** 660
13 Ruiz-Cabello, J., Vuister, G.W., Moonen, C.T.W., van Gelderen, P., Cohen, J.S., and van Zihl, P.C.M. *J. Magn. Reson.* 1992, **100,** 282
14 Kumar, A., Ernst, R.R., and Wüthrich, K. *Biochem. Biophys. Res. Commun.* 1980; **95,** 1
15 Bothner-By, A.A., Stephens, R.L., Lee, J.M., Warren, C.D., and Jeanloz, R.W. *J. Am. Chem. Soc.* 1984, **106,** 811
16 Hwang, T.L., and Shaka, A.J. *J. Am. Chem. Soc.* 1992, **114,** 3157
17 Stott, K., Stonehouse, J., Keeler, J., Hwang, T.-L., Shaka, A.J. *J. Am. Chem. Soc.* 1995, **117,** 4199
18 Haasnoot, C.A.G., de Leeuw, F.A.A.M., and Altona, C. *Tetrahedron* 1980, **36,** 2783
19 Neuhaus, D., and Williamson, M.P. *The nuclear Overhauser effect in structural and conformational analysis.* VCH, New York, 1989
20 (a) Homans, S.W. *Biochemistry* 1990, **29,** 9110. (b) Mukhopadhyay, C., Miller, K.E., and Bush, C.A. *Biopolymers* 1994, **34,** 21. (c) Rutherford, T.J., Partridge, J., Weller, C.T., and Homans, S.W. *Biochemistry* 1993, **32,** 12715. (d) Siebert, H.C., Reuter, G., Schauer, R., von der Lieth, C.W., and Dabrowski, J. *Biochemistry* 1992, **31,** 6962. (e) Engelsen, S.B., Herve du Penhoat, C., and Perez, S. *J. Phys. Chem.* 1995, **99,** 13334
21 (a) Lemieux, R.U., Koto, S., Voisin, D. *Am. Chem. Soc. Symp. Ser.* 1979 **87,** 17–29. (b) Thatcher, G.R.J. Thatcher. *The anomeric effect and associated stereoelectronic effects.* American Chemical Society, Washington, DC, 1993. (c) Kirby, A.J. *The anomeric effect and related stereoelectronic effects at oxygen.* Springer-Verlag, Heidelberg, Germany, 1983. (d) Thogersen, H., Lemieux, R.U., Bock, K., Meyer, B. *Can. J. Chem.* 1982, **60,** 44–65. (e) Tvaroska, I., Bleha, T. *Adv. Carbohydr. Chem. Biochem.* 1989, **47,** 45–103. (f) Wiberg, K.B., Murcko, M.A. *J. Am. Chem. Soc.* 1989, **111,** 4821–4827

Miguel A. Rodríguez-Carvajal, Manuel Bernabe, José L. Espartero, Pilar Tejero-Mateo, Antonio Gil-Serrano, and Jesús Jiménez-Barbero

Studies on the solution conformation and dynamics of a polysaccharide from *Sinorhizobium fredii* HH103 and its monosaccharide repeating unit

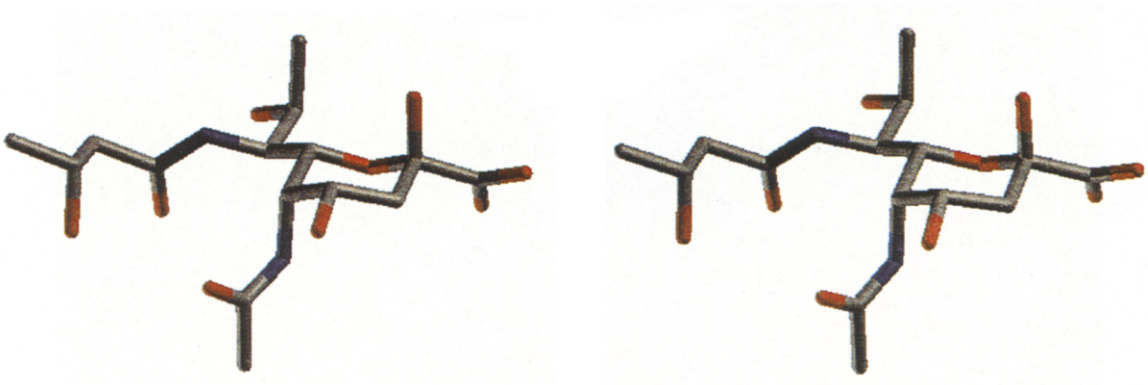

Color Plate 1. One of the possible low-enerty conformers of the monosaccharide, which is in agreement with the NMR data.

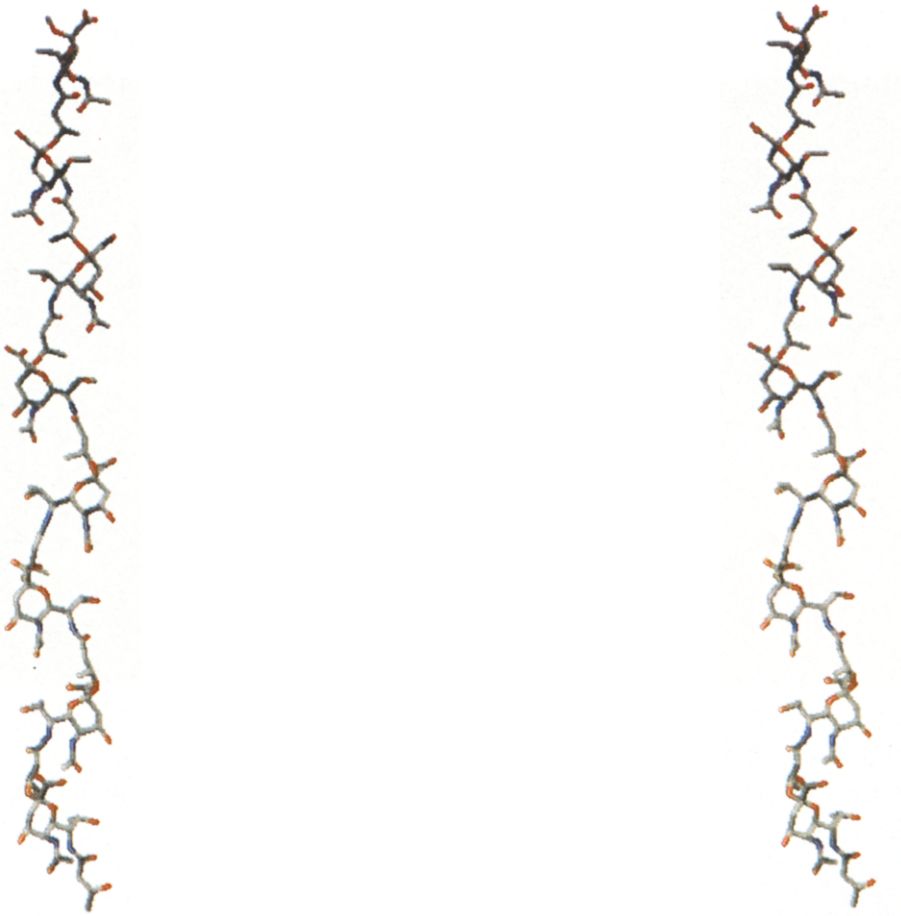

Color Plate 2. Stereoview of a possible conformation of an octasaccharide fragment carrying the *R*-configuration in the 3-hydroxybutyramido chains of the polysaccharide, which is in agreement with the NMR data.